

# Catalysis Science & Technology

Accepted Manuscript



This is an *Accepted Manuscript*, which has been through the Royal Society of Chemistry peer review process and has been accepted for publication.

*Accepted Manuscripts* are published online shortly after acceptance, before technical editing, formatting and proof reading. Using this free service, authors can make their results available to the community, in citable form, before we publish the edited article. We will replace this *Accepted Manuscript* with the edited and formatted *Advance Article* as soon as it is available.

You can find more information about *Accepted Manuscripts* in the [Information for Authors](#).

Please note that technical editing may introduce minor changes to the text and/or graphics, which may alter content. The journal's standard [Terms & Conditions](#) and the [Ethical guidelines](#) still apply. In no event shall the Royal Society of Chemistry be held responsible for any errors or omissions in this *Accepted Manuscript* or any consequences arising from the use of any information it contains.

**Size-dependent CO and Propylene Oxidation Activities of Platinum Nanoparticles on the Monolithic Pt/TiO<sub>2</sub>-YO<sub>x</sub> Diesel Oxidation Catalyst under Simulative Diesel Exhaust Conditions**

Zhengzheng Yang<sup>1</sup>, Jun Li<sup>2</sup>, Hailong Zhang<sup>2</sup>, Yi Yang<sup>2</sup>, Maochu Gong<sup>3,4</sup>, Yaoqiang Chen<sup>1,2,3,4\*</sup>

1 College of Architecture and Environment, Sichuan University, Chengdu 610064, Sichuan, PR China.

2 Key Laboratory of Green Chemistry & Technology of the Ministry of Education, College of Chemistry, Sichuan University, Chengdu 610064, Sichuan, PR China.

3 Sichuan Provincial Vehicular Exhaust Gases Abatement Engineering Technology Center, Chengdu 610064, Sichuan, PR China.

4 Sichuan Provincial Environmental Protection Environmental Catalytic Materials Engineering Technology Center, Chengdu 610064, Sichuan, PR China.

\*Corresponding author: Yaoqiang Chen

E-mail: nic7501@scu.edu.cn

Tel./Fax: +86 28 85418451

**Abstract:** In this work, we determined the CO and C<sub>3</sub>H<sub>6</sub> oxidation rates on size-selected Pt nanoparticles (1 nm ultrafine size and 8.8 nm nanoscale size average in diameters) deposited on TiO<sub>2</sub>-YO<sub>x</sub> supports. Both Pt/TiO<sub>2</sub>-YO<sub>x</sub> catalysts were characterized by transmission electron microscopy (TEM), X-ray photoelectron spectroscopy (XPS) and H<sub>2</sub> temperature-programmed reduction (H<sub>2</sub>-TPR). Results show that platinum particles on the fresh as-synthesized catalysts are fully oxidized to PtO<sub>2</sub> during the calcining in air; part of PtO<sub>2</sub> can be regenerated to Pt<sup>0</sup> active phase under the oxygen rich diesel exhaust conditions (containing about 1000 ppm CO), in which the ultrafine Pt particles supplying larger surface to volume ratio are beneficial for Pt<sup>0</sup> regeneration than the nanoscale ones. Such regeneration of Pt<sup>0</sup> existed even in oxygen rich diesel exhaust conditions leads to a significantly better global catalytic performance for the DOC reaction. Thus this work suggests that Pt<sup>0</sup> occupation ratio under the DOC reaction conditions may become a criteria to identify the quality of the DOC catalysts.

**Keywords:** platinum metal regeneration, surface to volume ratio, vehicular emissions, aftertreatment system

## 1. Introduction

Platinum supported catalysts are widespread application for gaseous phase catalytic oxidation. Ultrafine platinum particles are well known to efficiently enhance the catalytic oxidation activity,<sup>1-5</sup> which are resulting from the cluster size effect or structure sensitivity.<sup>3, 6, 7</sup>

For the diesel exhaust gases purification catalysts, due to the large oxygen excess,<sup>8-11</sup> the smaller platinum particles are much more easily oxidized to form platinum oxides under oxidizing atmosphere and hence platinum metal active components loss, which results in the catalytic performance decrease.<sup>12-15</sup> Relatively larger platinum particles maintain platinum metal state more easily under oxidizing atmosphere, hence supply more platinum metal active sites and better catalytic performance for NO, CO, C<sub>3</sub>H<sub>6</sub> oxidation.<sup>13-15</sup> Whereas, recent studies revealed that smaller platinum cluster can provide larger surface to volume ratio and more surface platinum atoms to involve in the reaction,<sup>16-18</sup> which would be favorable for Pt reactivity; and researches regarding diesel oxidation catalyst (DOC) aging also indicate that platinum particles growth is a detrimental influence for the DOC catalytic reaction (oxidizing CO, C<sub>3</sub>H<sub>6</sub> and partial NO) under real diesel engine exhaust conditions.<sup>19-21</sup> Therefore, designing the most efficient and stable Pt particles with optimal size is an important issue in purifying the real diesel exhaust.

However, the effects of Pt particle size and reaction environment on the active phase state and reactivity of real monolithic DOC catalysts at diesel exhaust conditions are still scarce. Our very recent study suggested that the smaller Pt

particles on the monolithic Pt/TiO<sub>2</sub>-YO<sub>x</sub> catalyst are favourable to the DOC reactivity at simulative diesel exhaust conditions.<sup>22</sup> Another paper demonstrates that the best catalytic performance in DOC reaction is resulting from an intermediate size of Pt particle, rather than the smallest size.<sup>23</sup> Does there exist a fundamental criteria for choosing the unique Pt particle size? Hence, in this study Pt size dependent activity for the DOC reaction under real technical monolithic catalyst were continuously investigated at the diesel exhaust conditions; considering the requirement of sulfur resistibility for DOCs in developing countries, the TiO<sub>2</sub> based support with excellent sulfur resistibility<sup>22, 24, 25</sup> was applied in this work. And we dedicate to figure out the effects of Pt particle size on the activity of CO and C<sub>3</sub>H<sub>6</sub> oxidation using real technical monolithic DOC catalysts at oxygen rich diesel exhaust conditions, focusing on the relationship between Pt particle size and size-activity, identifying the chemical states of Pt active species for the relevant CO and C<sub>3</sub>H<sub>6</sub> reactions.

## 2. Experimental

### 2.1. Catalyst preparation

#### 2.1.1. Powder catalyst

Pt/TiO<sub>2</sub>-YO<sub>x</sub> catalyst with ultrafine platinum particles (~1 nm), marked as U-Pt/TiO<sub>2</sub>-YO<sub>x</sub>, was synthesized using the approach reported in our recent work<sup>22</sup> and briefly described as follows. TiO<sub>2</sub>-YO<sub>x</sub> mixed oxides supports were prepared by co-precipitation method, TiOSO<sub>4</sub> and Y(NO<sub>3</sub>)<sub>3</sub> mixture solutions with a molar ratio of Ti : Y = 9 : 1 were slowly added into NH<sub>3</sub>·H<sub>2</sub>O solutions under vigorous stirring,

the precipitate was filtered and washed many times, then dried overnight and calcined for 3 h at 500 °C under airflow. After that,  $(EA)_2Pt(OH)_6$  solution was impregnated on the  $TiO_2-YO_x$  mixed oxides supports with a mass ratio of Pt :  $TiO_2-YO_x$  = 1.0%, after drying at 120 °C for 2 h and baking at 400 °C for 2 h under airflow, U-Pt/ $TiO_2-YO_x$  catalyst powder was obtained.

Pt/ $TiO_2-YO_x$  catalyst with nanoscale platinum particles (about 8.8 nm), labeled as Pt/ $TiO_2-YO_x$ , was prepared by calcining the U-Pt/ $TiO_2-YO_x$  powder catalyst at 700 °C for 5 h under airflow,<sup>15</sup> so as to avoid the effects resulting from diverse preparation pathways and ensure the same platinum loading.

#### 2.1.2. Monolithic catalyst

The monolithic U-Pt/ $TiO_2-YO_x$  catalyst was prepared by coating the slurry of U-Pt/ $TiO_2-YO_x$  catalyst powder onto a ceramic honeycomb (400 channels per square inch, 6 mill) with a washcoat loading of 120 g·L<sup>-1</sup>. And the Pt/ $TiO_2-YO_x$  monolithic catalyst was obtained by calcining the U-Pt/ $TiO_2-YO_x$  monolith at 700 °C for 5 h under airflow.

#### 2.1.3. Pre-reacted catalyst

To investigate the state of catalysts in the reaction process, the catalysts were pre-reacted under the simulative diesel exhaust gases (containing 1000 ppm CO, 330 ppm C<sub>3</sub>H<sub>6</sub>, 200 ppm NO, 50 ppm SO<sub>2</sub>, 8% CO<sub>2</sub>, 7% water vapor, 10% O<sub>2</sub>, and N<sub>2</sub> balance<sup>26</sup>) at 500 °C for 3 h, marked as U-Pt/ $TiO_2-YO_x$ (3h rea.) and Pt/ $TiO_2-YO_x$ (3h rea.), and then detected.

## 2.2 Catalytic activity measurements

The catalytic performance measurements were performed in a continuous flow fixed bed reactor. The monolithic catalysts were placed in a quartz tube reactor with an electric heater. The simulative diesel exhaust gases<sup>26</sup> contained a mixture of 1000 ppm CO, 330 ppm C<sub>3</sub>H<sub>6</sub>, 200 ppm NO, 50 ppm SO<sub>2</sub>, 8% CO<sub>2</sub>, 7% water vapor, 10% O<sub>2</sub>, and N<sub>2</sub> balance at a gas space velocity of 60 000 h<sup>-1</sup>. The inlet gas temperature was measured by a K-thermocouple which was fixed 20 mm in front of the monolith to avoid the effect of oxidation reactions (exothermic) on the inlet gas temperature. Another 0.5 mm K-thermocouple, in the middle of one of the center channels inside the monolith catalyst, was used to measure the catalyst bed temperature.

The outlet CO was detected using an FGA-4100 automotive emission analyzer (Foshan Analytical Instrument Co., Ltd., China), C<sub>3</sub>H<sub>6</sub> was analyzed with a GC2000II online gas chromatograph (Shanghai Analysis Instruments, China) using a flame ionization detector (FID), NO and NO<sub>2</sub> were detected by FT-IR (Antaris IGS Analyzer, Thermo Scientific, USA).

### 2.3. Catalyst Characterization

The particle size of catalysts were observed using a transmission electron microscopy (TEM) Tecnai G<sup>2</sup> F20 (E. A. Fischione Instruments Inc., USA).

X-ray photoelectron spectroscopy (XPS) data were collected on a Kratos XSAM 800 spectroscopy (Kratos Analytic Inc.) with Al K $\alpha$  radiation, C1s binding energy (BE 284.8 eV) was used to calibrate the binding energy shifts of samples.

The H<sub>2</sub> temperature-programmed reduction (H<sub>2</sub>-TPR) experiments were performed in a quartz tubular reactor. Samples (0.1 g) were pretreated in a flow of N<sub>2</sub> (35

mL/min) at 450 °C for 1 h. After cooling to room temperature, the reduction reaction was performed in a flow of H<sub>2</sub> (5.0 vol.%)–N<sub>2</sub> mixture (20 mL/min) from room temperature to 800 °C with a heating rate of 10 °C/min. The hydrogen consumption as a function of reduction temperature was monitored with a thermal conductivity detector (TCD) cell and recorded. The apparatus was calibrated by the reduction of pure CuO.

CO chemisorption on Pt was performed at room temperature in a quartz tubular reactor. Before CO chemisorption the samples were first heated to 500 °C in a hydrogen flow (H<sub>2</sub>, 99.999%) of 50 mL/min and exposed for 2 h. After rapidly cooling to room temperature in the same reducing stream, helium (He, 99.999%) flowed through the catalyst for 10 min. And then, the Pt dispersions of different catalysts were determined by CO chemisorption, and a factor of 0.8 CO/Pt was used to calculate the exposed surface Pt atoms due to CO can bind linearly and bridged<sup>27,</sup>

<sup>28</sup>.

### 3. Results and discussion

#### 3.1. Catalyst characterization

##### 3.1.1. Platinum particle size

Fig. 1a and b show the high-angle annular dark-field scanning transmission electron microscopy (HAADF-STEM) images of U-Pt/TiO<sub>2</sub>-YO<sub>x</sub>(3h rea.) and Pt/TiO<sub>2</sub>-YO<sub>x</sub>(3h rea.) catalysts, Fig. 1c shows high resolution transmission electron microscopy (HR-TEM) image of the U-Pt/TiO<sub>2</sub>-YO<sub>x</sub>(3h rea.). The platinum particle



size distribution over U-Pt/TiO<sub>2</sub>-YO<sub>x</sub>(3h rea.) and Pt/TiO<sub>2</sub>-YO<sub>x</sub>(3h rea.) catalysts are counted and shown in Fig. 1d. It can be seen that, platinum particles over the U-Pt/TiO<sub>2</sub>-YO<sub>x</sub>(3h rea.) catalyst are mainly distributed in the range of 0.4-1.0 nm with a mean diameter of 0.77 nm, which suggests that the average platinum particle contains about 14 platinum atoms (crude sphere model, platinum atomic radius is 0.14 nm<sup>29</sup>), it is believed that the ultrafine platinum particles (~1 nm) shows a flatter geometry (with only two atomic layers), that is, virtually all of the Pt atoms are surface atoms,<sup>17</sup> surface to volume ratio is about 0.92; for the Pt/TiO<sub>2</sub>-YO<sub>x</sub>(3h rea.) catalyst, the platinum particle size distribution ranges between 6 and 11nm with a mean size of 8.8 nm (roughly 21 000 platinum atoms), which implies that the platinum particle shows approximately 28 atomic layers and 0.19 surface to volume ratio. Through the aforementioned analysis, it can be suggested that each gram of the U-Pt/TiO<sub>2</sub>-YO<sub>x</sub>(3h rea.) catalyst contains about  $2.93 \times 10^{19}$  surface Pt atoms, which approximately presents an increase by a factor of 5 compared with the Pt/TiO<sub>2</sub>-YO<sub>x</sub>(3h rea.) catalyst ( $0.61 \times 10^{19}$  surface Pt atoms) in the case of same platinum loading; in essence, the U-Pt/TiO<sub>2</sub>-YO<sub>x</sub>(3h rea.) catalyst with smaller Pt particles (larger surface to volume ratio) possess significantly more potential active sites (surface Pt atoms),<sup>17, 18</sup> and hence better catalytic reactivity.

### 3.1.2. Platinum chemical states

Platinum chemical states of the catalysts were determined by XPS, as shown in Fig. 2, both the U-Pt/TiO<sub>2</sub>-YO<sub>x</sub> and Pt/TiO<sub>2</sub>-YO<sub>x</sub> catalysts show the 4f<sub>7/2</sub> peak position of

PtO<sub>2</sub> at around 74.8 eV with a spin-orbit splitting (PtO<sub>2</sub> 4f<sub>5/2</sub>) at 78.2 eV, which implies that the platinum particles over the fresh synthesized catalysts are fully oxidized to form PtO<sub>2</sub> due to the high temperature calcination process under airflow. After three hours pre-reaction under the simulative diesel exhaust gases, the PtO<sub>2</sub> over U-Pt/TiO<sub>2</sub>-YO<sub>x</sub> and Pt/TiO<sub>2</sub>-YO<sub>x</sub> catalysts are reduced to different levels. The U-Pt/TiO<sub>2</sub>-YO<sub>x</sub>(3h rea.) shows four peaks around 74.8 and 78.2 eV, assigned to 4f<sub>7/2</sub> and 4f<sub>5/2</sub> peaks of PtO<sub>2</sub>, as well as 70.9 and 74.3 eV, referring to 4f<sub>7/2</sub> and 4f<sub>5/2</sub> peaks of Pt metal, the content of Pt metal in total platinum species is about 15.8%, which indicates that ultrafine PtO<sub>2</sub> particles can be reduced to form Pt<sup>0</sup> under the diesel exhaust (containing trace amounts of CO and NO etc.) even if it is oxygen-rich condition.<sup>12</sup> While, for the Pt/TiO<sub>2</sub>-YO<sub>x</sub>(3h rea.) catalyst, the content of Pt<sup>0</sup> in total platinum species is just approximately 5% at the most, and two inconspicuous peaks around 73.9 (PtO 4f<sub>7/2</sub>) and 77.3 eV (PtO 4f<sub>5/2</sub>) show that about 2% Pt<sup>2+</sup> may be formed after three hours DOC reduction, which demonstrates that larger size PtO<sub>2</sub> particles also can be reduced to different degrees under the diesel exhaust, but the production of Pt<sup>0</sup> is remarkably less than that of ultrafine PtO<sub>2</sub> particles. The U-Pt/TiO<sub>2</sub>-YO<sub>x</sub> catalyst with a 0.92 surface to volume ratio produces 5.04×10<sup>18</sup> Pt<sup>0</sup> atoms per gram catalyst after running 3 hours DOC reaction, for the Pt/TiO<sub>2</sub>-YO<sub>x</sub> (surface to volume ratio is 0.19), the 3 hours DOC reaction results in production of 1.59×10<sup>18</sup> Pt<sup>0</sup> atoms per gram catalyst; which indicates that in reaction process the U-Pt/TiO<sub>2</sub>-YO<sub>x</sub> catalyst with smaller Pt particle (higher surface to volume ratio) can provide more Pt<sup>0</sup> active sites to involve in the reaction. According to the above results,

it can be suggested that  $\text{PtO}_2$  particles can be reduced to  $\text{Pt}^0$  in the oxygen rich diesel exhaust; the smaller size is beneficial for supplying more surface Pt atoms ( $\text{Pt}^{4+}$ ) to involve in the reaction forming  $\text{Pt}^0$  species, and hence improved the catalytic activity on account of that  $\text{Pt}^0$  is more active than platinum oxides for the diesel exhaust oxidation reactions.<sup>12-14</sup>

### 3.1.3. Platinum reduction property

The catalyst with excellent reduction property is favourable for effectively purifying CO and hydrocarbons in exhaust gases.<sup>30</sup> The effects of ultrafine size platinum on the catalyst reduction property were measured by hydrogen temperature-programmed reduction ( $\text{H}_2$ -TPR). The as-synthesized supports and catalysts (before pre-reaction) were used for the  $\text{H}_2$ -TPR measurements. Fig. 3 clearly shows that, the  $\text{TiO}_2$ - $\text{YO}_x$  supports are reduced at around 500-650 °C, the peak shape and position are slightly changed when platinum was supported on the supports; the U-Pt/ $\text{TiO}_2$ - $\text{YO}_x$  catalyst, platinum particle mean size is 0.77 nm, shows two conspicuous hydrogen consumption peaks before 200 °C, which illustrates that the U-Pt/ $\text{TiO}_2$ - $\text{YO}_x$  catalyst with ultrafine size  $\text{PtO}_2$  shows excellent low temperature reducing property; for the Pt/ $\text{TiO}_2$ - $\text{YO}_x$  catalyst, mean size of platinum is 8.8 nm, the peaks before 200 °C are very weak and a broad reduction peak arises until the temperature rise to about 300 °C, which suggest that compare to the U-Pt/ $\text{TiO}_2$ - $\text{YO}_x$ , the Pt/ $\text{TiO}_2$ - $\text{YO}_x$  with larger  $\text{PtO}_2$  particles show worse low temperature reduction property.

To analyze the catalysts reduction property in detail, all H<sub>2</sub>-TPR peaks information were counted and listed in Table 1. It can be seen that the total H<sub>2</sub>-consumption of U-Pt/TiO<sub>2</sub>-YO<sub>x</sub> is 136 μmol which is consistent with that of Pt/TiO<sub>2</sub>-YO<sub>x</sub> catalyst (148 μmol), the total H<sub>2</sub>-consumption of TiO<sub>2</sub>-YO<sub>x</sub> supports are 146 μmol, the small differences result from the weighing deviation of samples. The calculated PtO<sub>2</sub> H<sub>2</sub>-consumption of the samples (0.1 g) are 10.25 μmol. The H<sub>2</sub>-consumption of U-Pt/TiO<sub>2</sub>-YO<sub>x</sub> catalyst at approximately 80 °C (peak I) is about 8.63 μmol. Taking XPS results, which show Pt<sup>2+</sup> is not existed in the incomplete reduction U-Pt/TiO<sub>2</sub>-YO<sub>x</sub> catalyst, into consideration, the peak I of U-Pt/TiO<sub>2</sub>-YO<sub>x</sub> catalyst can be associated with the one step reduction of surface Pt<sup>4+</sup> to Pt metal;<sup>31</sup> due to most of surface Pt species are reduced before 150 °C, the peak II at about 175 °C may results from the effect of strong metal-support interactions (SMSI),<sup>32-34</sup> reduction of TiO<sub>2</sub>-YO<sub>x</sub> supports through the strong interaction with platinum,<sup>31</sup> other researches also indicated that TiO<sub>2</sub> can be reduced at about 180 °C when platinum was supported on TiO<sub>2</sub>.<sup>35, 36</sup> For the Pt/TiO<sub>2</sub>-YO<sub>x</sub> catalyst, the peak I and II are extremely weak, and an evident reduction peak, peak III, arises at approximately 300 °C with about 7.55 μmol H<sub>2</sub>-consumption which is close to the total PtO<sub>2</sub> H<sub>2</sub>-consumption, researchers reported that bulk PtO<sub>2</sub> decompose at about 300 °C,<sup>36, 37</sup> hence, we associated the peak III with bulk PtO<sub>2</sub> reduction.

Based on the above discussion, it can be suggested that the reduction of ultrafine size PtO<sub>2</sub> particles are mainly for surface reduction, which are easily reacted at low temperature, furthermore due to that Pt on TiO<sub>2</sub> support displays SMSI,<sup>32-34</sup> the

interface supports through strong interaction with ultrafine platinum are also plentifully reduced at low temperature. However, the reduction for larger size PtO<sub>2</sub> particles are mainly for bulk reduction, which are reacted at a higher temperature. Thus, it can be inferred that the ultrafine size platinum particles of U-Pt/TiO<sub>2</sub>-YO<sub>x</sub> catalyst are more easily involved into the catalytic reaction at low temperature, and hence better low temperature catalytic performance.

### 3.2. Catalytic performance

Fig. 4 shows C<sub>3</sub>H<sub>6</sub> (a) and CO (b) conversion over the as-synthesized and pre-reacted catalysts. For C<sub>3</sub>H<sub>6</sub> combustion, the U-Pt/TiO<sub>2</sub>-YO<sub>x</sub>, Pt/TiO<sub>2</sub>-YO<sub>x</sub> and Pt/TiO<sub>2</sub>-YO<sub>x</sub>(3h rea.) catalysts show similar activity at high conversion, which may since C<sub>3</sub>H<sub>6</sub> combustion reaction is strongly temperature dependent,<sup>38</sup> and the U-Pt/TiO<sub>2</sub>-YO<sub>x</sub>(3h rea.) shows better activity at the same inlet gas temperature may be owing to CO low temperature light-off increased the catalyst bed temperature. For CO oxidation, the U-Pt/TiO<sub>2</sub>-YO<sub>x</sub> shows slightly better catalytic performance than that of the Pt/TiO<sub>2</sub>-YO<sub>x</sub> catalyst; after 3 h pre-reaction under the simulative diesel exhaust gases (before measuring the catalytic performance, industrial DOC must be pre-reacted under the diesel vehicle exhaust to stable the catalyst state), both the U-Pt/TiO<sub>2</sub>-YO<sub>x</sub>(3h rea.) and Pt/TiO<sub>2</sub>-YO<sub>x</sub>(3h rea.) catalysts show significantly better activity than the catalyst without pre-reaction, due to plenty of platinum metal active phase were produced in the pre-reaction process (Fig. 2), and the U-Pt/TiO<sub>2</sub>-YO<sub>x</sub>(3h rea.) catalyst shows noticeably better catalytic activity than the Pt/TiO<sub>2</sub>-YO<sub>x</sub>(3h rea.)

catalyst, which results from ultrafine platinum oxide particles of the U-Pt/TiO<sub>2</sub>-YO<sub>x</sub> are more easily reduced (as shown in Fig. 3) to form more Pt<sup>0</sup> active phase in the pre-reaction process under the simulative diesel exhaust (Fig. 2) and involved into the reaction, hence obviously better catalytic performance. In essence, this result is consistent with the view that the larger platinum particles of catalysts remaining platinum metal active phase more easily under oxidizing atmosphere (without CO) shows better oxidation activity.<sup>13, 14, 39</sup> Experimental results indicate the ultrafine platinum particle is beneficial for the regeneration of Pt<sup>0</sup> under diesel exhaust conditions and hence improving DOC catalytic activity. Note that high temperature calcining was used to prepare the nanoscale size Pt/TiO<sub>2</sub>-YO<sub>x</sub> catalyst which might affect the catalyst texture and hence activity. On account of that, an additional N<sub>2</sub> adsorption-desorption measurement was employed, as is shown in Table 2, the surface area of Pt/TiO<sub>2</sub>-YO<sub>x</sub>(3h rea.) decreased in the process of high temperature preparation, but the pore volume kept stable; which indicates that the porous texture of Pt/TiO<sub>2</sub>-YO<sub>x</sub>(3h rea.) catalyst were not destroyed and hence the effects of textural properties for the catalytic performance of Pt/TiO<sub>2</sub>-YO<sub>x</sub>(3h rea.) are not fateful. Therefore, it can be safely concluded that the ultrafine size of platinum particle is one of the most important favorable reasons for the DOC catalytic reaction. Additionally, it should be mentioned that these results do not indicate that the smaller the platinum particle size, the better the reaction activity, which is proved by Boubnov et al.,<sup>23</sup> due to the ripening or even sintering of Pt cluster in the reaction process.<sup>18, 40, 41</sup>

To further clarify the catalytic performance differences, the activation energies

were determined by using the Arrhenius equation. The low temperature range that resulted in low  $C_3H_6$  and CO conversion (less than 15%) was used to calculate  $C_3H_6$  and CO oxidation reactions activation energies, so as to maintain kinetically limited and avoid mass transfer limitation complications.<sup>42</sup> The dispersion of platinum were measured by CO chemisorption, and the factor of 0.8 CO/Pt was used to calculate the exposed Pt atoms due to CO can bind linearly and bridged,<sup>27, 28</sup> dispersion of platinum atoms of the U-Pt/TiO<sub>2</sub>-YO<sub>x</sub> and Pt/TiO<sub>2</sub>-YO<sub>x</sub> catalysts are about 30.85% and 6.35%, respectively. The coefficient of determination ( $R^2$ ) for all Arrhenius plots were at least 0.97. Calculated activation energies and reaction rates results are listed in Table 3. The activation energies of  $C_3H_6$  combustion over the pre-reacted catalysts containing platinum metal (both U-Pt/TiO<sub>2</sub>-YO<sub>x</sub>(3h rea.) and Pt/TiO<sub>2</sub>-YO<sub>x</sub>(3h rea.)) are lower than that over the fresh as-synthesized samples (U-Pt/TiO<sub>2</sub>-YO<sub>x</sub> and Pt/TiO<sub>2</sub>-YO<sub>x</sub>, without Pt<sup>0</sup>); the U-Pt/TiO<sub>2</sub>-YO<sub>x</sub> shows similar activation energy as the Pt/TiO<sub>2</sub>-YO<sub>x</sub> catalyst, and this trend reproduces over the pre-reacted catalysts. Based on the above analysis, it can be inferred that platinum metal is beneficial for  $C_3H_6$  combustion and  $C_3H_6$  combustion probably is not size sensitive reaction in the kinetically limited range. Noteworthy, the reaction rate of  $C_3H_6$  combustion is inhibited by the presence of CO and NO under simulative engine exhaust,<sup>22, 43</sup> and hence affecting the kinetic parameters; however, the global reaction rate of  $C_3H_6$  combustion on the U-Pt/TiO<sub>2</sub>-YO<sub>x</sub>(3h rea.) catalyst at 210 °C (the low temperature range of diesel exhaust) is remarkably higher than that over the others catalysts in the simulative diesel exhaust, which demonstrates that ultrafine size platinum particles are favorable

for enhancing the purifying efficiency of  $C_3H_6$  in the practical use of DOC. For CO oxidation reaction, both pre-reacted samples show distinctly better catalytic performance than the fresh as-synthesized catalysts; the U-Pt/TiO<sub>2</sub>-YO<sub>x</sub> catalyst owning ultrafine size platinum particles shows lower activation energy and higher reaction rate than the Pt/TiO<sub>2</sub>-YO<sub>x</sub> catalyst, this trend is the same as the pre-reacted catalysts; which implies that ultrafine size platinum particles are significantly beneficial for improving the catalytic activity of CO oxidation under the diesel exhaust conditions. These results seem different from the opinion reported by Fridell and Olsson and Ribeiro et al. that larger particles of Pt increase the vehicle exhaust oxidation reactivity (for NO).<sup>13, 14, 39</sup> Since their researches are based on the de-NO<sub>x</sub> vehicle exhaust purifying catalyst which is placed after DOC and worked under the oxidizing atmosphere (CO etc. reducing gases have been removed by the DOC), larger Pt particles are favorable for maintaining Pt<sup>0</sup> active sites un-oxidized under the oxidizing atmosphere, and hence catalyst with larger Pt particles shows better reactivity;<sup>13, 14, 39</sup> and our results imply that smaller Pt oxides particles are more easily reduced by the original diesel exhaust (containing trace amounts of CO etc. reducing gases) forming Pt<sup>0</sup> active phase, which is in essence consistent with their results.

Besides the CO and  $C_3H_6$  catalytic reactivity, the NO oxidation performance was also measured. As is shown in Fig. 5, the after pre-reacted samples (both U-Pt/TiO<sub>2</sub>-YO<sub>x</sub>(3h rea.) and Pt/TiO<sub>2</sub>-YO<sub>x</sub>(3h rea.)) displayed significantly better NO oxidation activity than the fresh samples, which results from the regeneration of Pt<sup>0</sup> active site in the pre-reaction process under simulative diesel exhaust gases. Due to



the different preparation batches and treatment conditions, the data values were a little different from our previous works, however the trends were the same.<sup>22</sup> For the fresh samples, at the beginning of reaction, the U-Pt/TiO<sub>2</sub>-YO<sub>x</sub> showed worse performance, which may due to the smaller Pt cluster would increase the chemisorbed oxygen concentration hence inhibit O<sub>2</sub> adsorption and NO oxidation;<sup>13</sup> after a certain time of reaction (at about 350 °C), the reactivity of U-Pt/TiO<sub>2</sub>-YO<sub>x</sub> was obviously improved, which results from the Pt<sup>0</sup> active phase regeneration in the reaction process.<sup>12</sup> After three hours pre-reaction, the U-Pt/TiO<sub>2</sub>-YO<sub>x</sub>(3h rea.) showed similar NO catalytic performance with the Pt/TiO<sub>2</sub>-YO<sub>x</sub>(3h rea.); due to the fact that the U-Pt/TiO<sub>2</sub>-YO<sub>x</sub>(3h rea.) displays smaller Pt particle size which would lead to worse NO reactivity; however, at the same time, the U-Pt/TiO<sub>2</sub>-YO<sub>x</sub>(3h rea.) shows more Pt<sup>0</sup> active sites which would result to better NO oxidation activity. The NO catalytic oxidation results indicate that the Pt particle size and Pt<sup>0</sup> production would affect the catalytic reactivity of NO oxidation simultaneously.

The relationship between Pt size-dependence and the DOC reactivity are listed in Table 4. It is clear that the catalyst with ultrafine size of Pt particles shows larger surface to volume ratio and more surface Pt atoms, and hence better catalytic activity; moreover, significantly more Pt<sup>0</sup> phase is produced on the U-Pt/TiO<sub>2</sub>-YO<sub>x</sub> catalyst after running 3 hours DOC reaction, and that further enhances the global C<sub>3</sub>H<sub>6</sub> and CO reaction rates under the diesel exhaust conditions. It is worth to note that Pt<sup>0</sup> can be more easily regenerated on the U-Pt/TiO<sub>2</sub>-YO<sub>x</sub> catalyst under even oxygen rich diesel exhaust condition. Chemical states of Pt can be critical to the DOC activity

based on the corresponding particle size. Therefore, the optimal Pt size still needs for further investigation. Pt<sup>0</sup> occupation ratio may become a criteria to identify the quality of the DOC catalysts.

#### 4. Conclusions

According to the abovementioned results, the conclusion can be reached that investigations of DOC reaction efficiency upon gaseous environment and catalyst size effect are both essential. Strong reducing gas traces (CO etc.) in real diesel exhaust are non-ignorable factors for the catalyst state and reaction activity; platinum oxides can be reduced to form Pt<sup>0</sup> active phase even if in the oxygen rich diesel exhaust gases (containing trace amounts of CO etc. reducing gases); the ultrafine size (~1 nm) of platinum particles supply an increase by a factor of about 5 for surface to volume ratio and surface Pt atoms compared with nanoscale size (8.8 nm) Pt particles, in which the ultrafine Pt particles are more favored to regenerate more Pt<sup>0</sup> active sites (more than 3 times), and end up with better CO and propylene purifying efficiency. Additionally, the DOC catalyst with ultrafine size platinum particles shows better catalytic performance under diesel exhaust conditions, which implies that maintaining the ultrafine size of platinum particles in a practical application would be an efficient approach to improve the high activity and durability of the catalysts; and Pt<sup>0</sup> occupation ratio under the DOC reaction conditions may become a criteria to identify the quality of the DOC catalysts.

## Acknowledgements

This work was supported by the Major Research Program of Sichuan Province Science and Technology Department (2012FZ0008), National Natural Science Foundation of China (21173153), and National High-Tech Research and Development Program of China (863) (2013AA065304).

## References

1. C. Nethravathi, E. Anumol, M. Rajamathi and N. Ravishankar, *Nanoscale*, 2011, 3, 569-571.
2. J. Lu and P. C. Stair, *Angewandte Chemie*, 2010, 49, 2547-2551.
3. S. Vajda, M. J. Pellin, J. P. Greeley, C. L. Marshall, L. A. Curtiss, G. A. Ballentine, J. W. Elam, S. Catillon-Mucherie, P. C. Redfern, F. Mehmood and P. Zapol, *Nature Materials*, 2009, 8, 213-216.
4. X. Li, W.-X. Chen, J. Zhao, W. Xing and Z.-D. Xu, *Carbon*, 2005, 43, 2168-2174.
5. Y. Takasu, H. Itaya, T. Iwazaki, R. Miyoshi, T. Ohnuma, W. Sugimoto and Y. Murakami, *Chem. Commun.*, 2001, 341-342.
6. D. Y. Murzin, *Catal Sci Technol*, 2014, 4, 3340-3350.
7. J. M. García-Cortés, J. Pérez-Ramírez, J. N. Rouzaud, A. R. Vaccaro, M. J. Illán-Gómez and C. Salinas-Martínez de Lecea, *J Catal*, 2003, 218, 111-122.
8. T. Kreuzer, E. S. Lox, D. Lindner and J. Leyrer, *Catal Today*, 1996, 29, 17-27.
9. M. V. Twigg, *Applied Catalysis B: Environmental*, 2007, 70, 2-15.
10. Z. Z. Yang, Y. D. Chen, M. Zhao, J. F. Zhou, M. C. Gong and Y. Q. Chen, *Chinese J Catal*, 2012, 33, 819-826.
11. Z.-Z. Yang, Y. Yang, M. Zhao, M.-C. Gong and Y.-Q. Chen, *Acta Phys-Chim Sin*, 2014, 30, 1187-1193.
12. K. Hauff, U. Tuttlies, G. Eigenberger and U. Nieken, *Applied Catalysis B: Environmental*, 2012, 123-124, 107-116.
13. A. D. Smeltz, W. N. Delgass and F. H. Ribeiro, *Langmuir*, 2010, 26, 16578-16588.
14. L. Olsson and E. Fridell, *J Catal*, 2002, 210, 340-353.
15. L. M. Carballo and E. E. Wolf, *J Catal*, 1978, 53, 366-373.
16. J. Wei and E. Iglesia, *The Journal of Physical Chemistry B*, 2004, 108, 4094-4103.
17. Y. Lei, H. Zhao, R. D. Rivas, S. Lee, B. Liu, J. Lu, E. Stach, R. E. Winans, K. W. Chapman, J. P. Greeley, J. T. Miller, P. J. Chupas and J. W. Elam, *J Am Chem Soc*, 2014, 136, 9320-9326.
18. S. Bonanni, K. Ait-Mansour, W. Harbich and H. Brune, *J Am Chem Soc*, 2014, 136, 8702-8707.
19. A. Winkler, D. Ferri and M. Aguirre, *Applied Catalysis B: Environmental*, 2009, 93, 177-184.
20. J. Andersson, M. Antonsson, L. Eurenus, E. Olsson and M. Skoglundh, *Applied Catalysis B: Environmental*, 2007, 72, 71-81.
21. F. C. Galisteo, C. Larese, R. Mariscal, M. L. Granados, J. Fierro, R. Fernández-Ruiz and M. Furio,

- Top Catal*, 2004, 30, 451-456.
22. Z. Yang, N. Zhang, Y. Cao, M. Gong, M. Zhao and Y. Chen, *Catal Sci Technol*, 2014, 4, 3032-3043.
  23. A. Boubnov, S. Dahl, E. Johnson, A. P. Molina, S. B. Simonsen, F. M. Cano, S. Helveg, L. J. Lemus-Yegres and J.-D. Grunwaldt, *Applied Catalysis B: Environmental*, 2012, 126, 315-325.
  24. H. Ueno, T. Furutani, T. Nagami, N. Aono, H. Goshima and K. Kasahara, *SAE Technical Paper*, 1998, 980195.
  25. T. Paulson, B. Moss, B. Todd, C. Eckstein, B. Wise, D. Singleton, S. Zemskova and R. Silver, *SAE Technical Paper*, 2008, 2008-01-2638.
  26. J. Kašpar, P. Fornasiero and N. Hickey, *Catal Today*, 2003, 77, 419-449.
  27. X. P. Auvray and L. Olsson, *Ind Eng Chem Res*, 2013, 52, 14556-14566.
  28. K. Foger and J. R. Anderson, *Applications of Surface Science*, 1979, 2, 335-351.
  29. J. C. Slater, *The Journal of Chemical Physics*, 1964, 41, 3199-3204.
  30. S. Park and C. Pak, *US Patent*, 1998, 5814577.
  31. S. S. Kim, K. H. Park and S. C. Hong, *Fuel Process Technol*, 2013, 108, 47-54.
  32. T. Huizinga, H. F. J. van 'T Blik, J. C. Vis and R. Prins, *Surf Sci*, 1983, 135, 580-596.
  33. H. G. Manyar, C. Paun, R. Pilus, D. W. Rooney, J. M. Thompson and C. Hardacre, *Chem Commun*, 2010, 46, 6279-6281.
  34. A. V. Kirilin, A. V. Tokarev, H. Manyar, C. Hardacre, T. Salmi, J. P. Mikkola and D. Y. Murzin, *Catal Today*, 2014, 223, 97-107.
  35. L. Wang, M. Sakurai and H. Kameyama, *J Hazard Mater*, 2009, 167, 399-405.
  36. P. Panagiotopoulou, A. Christodoulakis, D. I. Kondarides and S. Boghosian, *J Catal*, 2006, 240, 114-125.
  37. T. Huizinga, J. Van Grondelle and R. Prins, *Applied Catalysis*, 1984, 10, 199-213.
  38. I. V. Yentekakis, V. Tellou, G. Botzolaki and I. A. Rapakousios, *Applied Catalysis B: Environmental*, 2005, 56, 229-239.
  39. E. Fridell, A. Amberntsson, L. Olsson, A. Grant and M. Skoglundh, *Top Catal*, 2004, 30-31, 143-146.
  40. S. B. Simonsen, I. Chorkendorff, S. Dahl, M. Skoglundh, K. Meinander, T. N. Jensen, J. V. Lauritsen and S. Helveg, *J Phys Chem C*, 2012, 116, 5646-5653.
  41. X. Auvray, T. Pingel, E. Olsson and L. Olsson, *Applied Catalysis B: Environmental*, 2013, 129, 517-527.
  42. H. Oh, I. Pieta, J. Luo and W. Epling, *Top Catal*, 2013, 56, 1916-1921.
  43. S. E. Voltz, C. R. Morgan, D. Liederman and S. M. Jacob, *Ind. Eng. Chem. Prod. Res. Develop.*, 1973, 12, 294-301.

### Figure Captions

Fig. 1. HAADF-STEM images of (a) U-Pt/TiO<sub>2</sub>-YO<sub>x</sub>, (b) Pt/TiO<sub>2</sub>-YO<sub>x</sub> catalysts; HR-TEM image of (c) U-Pt/TiO<sub>2</sub>-YO<sub>x</sub> catalyst; (d) Pt particle size distribution of the both catalysts.

Fig.2. XPS (Pt 4f) spectra of the U-Pt/TiO<sub>2</sub>-YO<sub>x</sub> and Pt/TiO<sub>2</sub>-YO<sub>x</sub> catalysts before or after three hours pre-reaction

Fig.3. H<sub>2</sub>-TPR profiles of the TiO<sub>2</sub>-YO<sub>x</sub> support, U-Pt/TiO<sub>2</sub>-YO<sub>x</sub> and Pt/TiO<sub>2</sub>-YO<sub>x</sub> catalysts

Fig.4. C<sub>3</sub>H<sub>6</sub> (a) and CO (b) oxidation conversion over the U-Pt/TiO<sub>2</sub>-YO<sub>x</sub>, Pt/TiO<sub>2</sub>-YO<sub>x</sub> catalysts and three hours pre-reacted U-Pt/TiO<sub>2</sub>-YO<sub>x</sub>(3h rea.), Pt/TiO<sub>2</sub>-YO<sub>x</sub>(3h rea.) catalysts.

Feed gas composition: 1000 ppm CO, 330 ppm C<sub>3</sub>H<sub>6</sub>, 200 ppm NO, 50 ppm SO<sub>2</sub>, 8% CO<sub>2</sub>, 7% water vapor, 10% O<sub>2</sub>, N<sub>2</sub> balance, gas space velocity 60 000 h<sup>-1</sup>.

Fig. 5. NO oxidation conversion over the fresh as-synthesized and after pre-treated catalysts.

Feed gas composition: 1000 ppm CO, 330 ppm C<sub>3</sub>H<sub>6</sub>, 200 ppm NO, 50 ppm SO<sub>2</sub>, 8% CO<sub>2</sub>, 7% water vapor, 10% O<sub>2</sub>, N<sub>2</sub> balance, gas space velocity 60 000 h<sup>-1</sup>.

Table 1. H<sub>2</sub>-TPR peaks information of the U-Pt/TiO<sub>2</sub>-YO<sub>x</sub> and Pt/TiO<sub>2</sub>-YO<sub>x</sub> catalysts

Peaks	U-Pt/TiO <sub>2</sub> -YO <sub>x</sub>			Pt/TiO <sub>2</sub> -YO <sub>x</sub>		
	Temperature (°C)	Areas	H <sub>2</sub> consumption (μmol)	Temperature (°C)	Areas	H <sub>2</sub> consumption (μmol)
I	50-140	33.2	8.63	110-160	1.01	0.26
II	140-230	32.7	8.48	190-260	1.13	0.29
III	260-280	1.0	0.25	270-350	29.1	7.55
IV-V	300-700	457	119	350-650	539	140
Total		524	136		570	148

Table 2. Texture properties of the U-Pt/TiO<sub>2</sub>-YO<sub>x</sub>(3h rea.) and Pt/TiO<sub>2</sub>-YO<sub>x</sub>(3h rea.).

Sample	Surface area (m <sup>2</sup> /g)	Pore volume (cm <sup>3</sup> /g)
U-Pt/TiO <sub>2</sub> -YO <sub>x</sub> (3h rea.)	138	0.31
Pt/TiO <sub>2</sub> -YO <sub>x</sub> (3h rea.)	64	0.30

Table 3. C<sub>3</sub>H<sub>6</sub> and CO oxidation reaction rates and activation energies over the U-Pt/TiO<sub>2</sub>-YO<sub>x</sub>, Pt/TiO<sub>2</sub>-YO<sub>x</sub> catalysts and three hours pre-reacted U-Pt/TiO<sub>2</sub>-YO<sub>x</sub>(3h rea.), Pt/TiO<sub>2</sub>-YO<sub>x</sub>(3h rea.) catalysts.

Reactions	Catalysts	Reaction rates(mol g <sup>-1</sup> s <sup>-1</sup> )	TOF (s <sup>-1</sup> )	Ea(kJ mol <sup>-1</sup> )
C <sub>3</sub> H <sub>6</sub> +O <sub>2</sub> <sup>a</sup>	U-Pt/TiO <sub>2</sub> -YO <sub>x</sub>	2.52×10 <sup>-7</sup>	0.0528	382.3
	Pt/TiO <sub>2</sub> -YO <sub>x</sub>	2.13×10 <sup>-7</sup>	0.2173	376.3
	U-Pt/TiO <sub>2</sub> -YO <sub>x</sub> (3h rea.)	19.7×10 <sup>-7</sup>	0.4146	246.7
	Pt/TiO <sub>2</sub> -YO <sub>x</sub> (3h rea.)	4.19×10 <sup>-7</sup>	0.4283	232.9
CO+O <sub>2</sub> <sup>b</sup>	U-Pt/TiO <sub>2</sub> -YO <sub>x</sub>	1.20×10 <sup>-6</sup>	0.2525	140.6
	Pt/TiO <sub>2</sub> -YO <sub>x</sub>	0.76×10 <sup>-6</sup>	0.7827	308.1
	U-Pt/TiO <sub>2</sub> -YO <sub>x</sub> (3h rea.)	4.76×10 <sup>-6</sup>	1.0023	104.3
	Pt/TiO <sub>2</sub> -YO <sub>x</sub> (3h rea.)	3.01×10 <sup>-6</sup>	3.0756	163.4

<sup>a</sup> Catalyst bed temperature is 210 °C. <sup>b</sup> Catalyst bed temperature is 200 °C.

Table 4. Relationship between Pt particle properties and the catalytic activity on the U-Pt/TiO<sub>2</sub>-YO<sub>x</sub> and Pt/TiO<sub>2</sub>-YO<sub>x</sub> catalysts.

Characters	U-Pt/TiO <sub>2</sub> -YO <sub>x</sub>	Pt/TiO <sub>2</sub> -YO <sub>x</sub>
Pt particle mean size	0.77 nm	8.8 nm
Pt surface to volume ratio	0.92	0.19
Surface Pt atoms per gram catalyst	2.93×10 <sup>19</sup>	0.61×10 <sup>19</sup>
CO molecules/(s Pt atom) <sup>a</sup>	0.0779	0.0494
C <sub>3</sub> H <sub>6</sub> molecules/(s Pt atom) <sup>a</sup>	0.0038	0.0021
After running 3 hours DOC reaction		
Pt <sup>0</sup> atoms per gram catalyst	5.04×10 <sup>18</sup>	1.59×10 <sup>18</sup>
CO molecules/(s Pt atom) <sup>a</sup>	0.3092	0.1953
C <sub>3</sub> H <sub>6</sub> molecules/(s Pt atom) <sup>a</sup>	0.0597	0.0137

<sup>a</sup> Inlet gas temperature is 200 °C.

Fig. 1

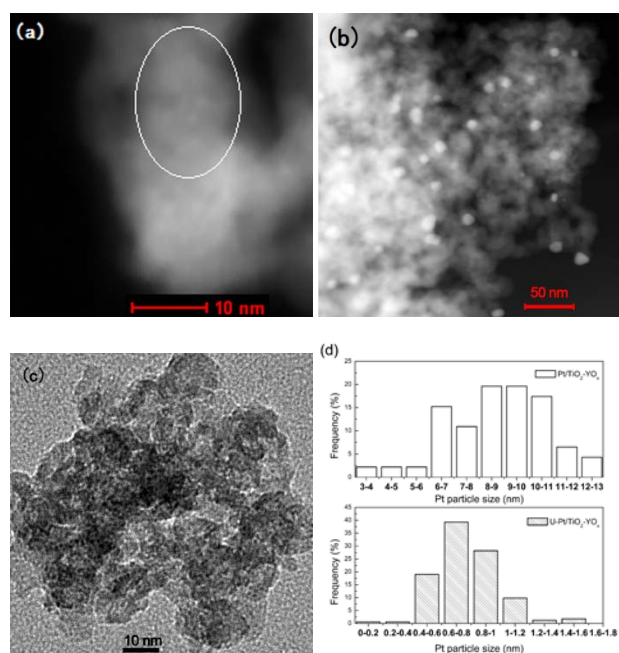




Fig. 2

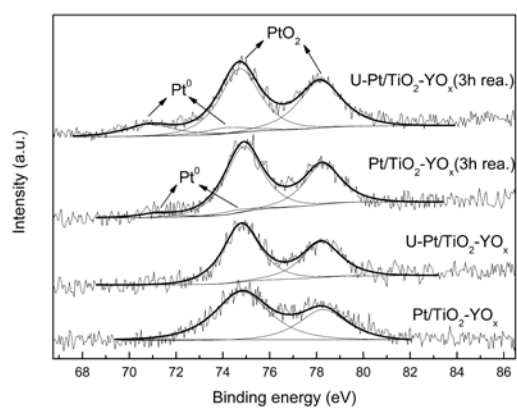


Fig. 3

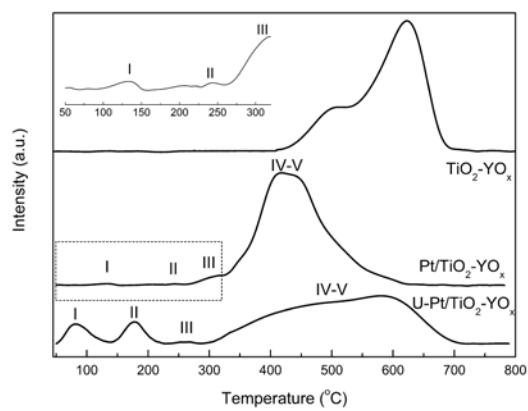


Fig. 4

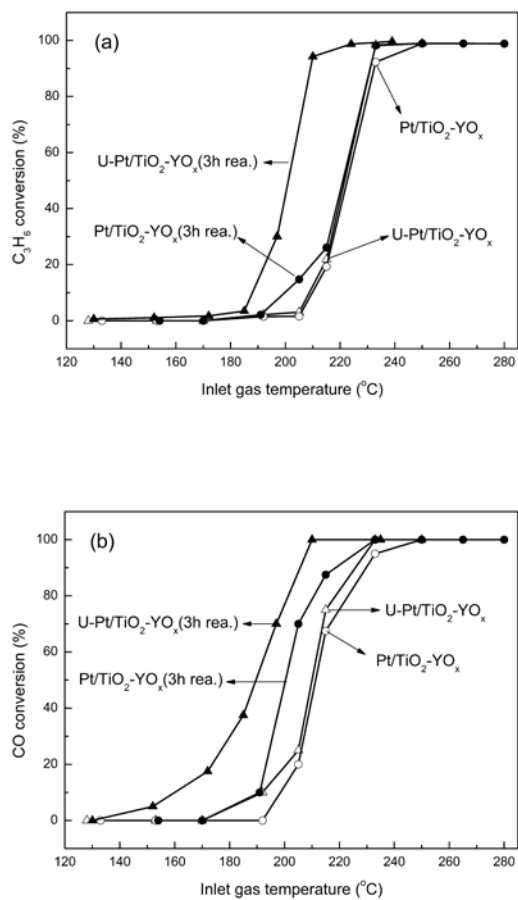
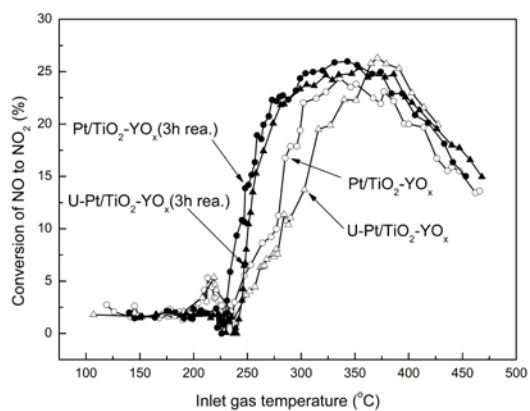
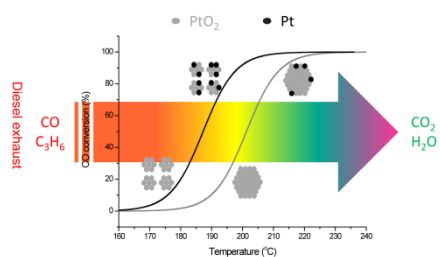


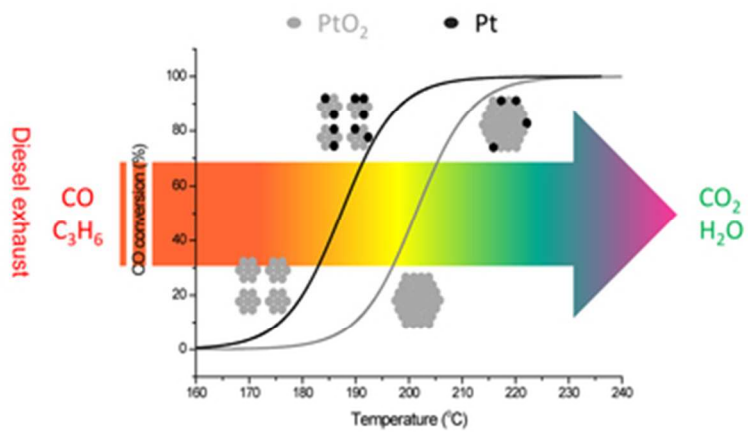
Fig. 5



## Graphical abstract



Small platinum oxides particles are beneficial for forming Pt<sup>0</sup> active species at the diesel exhaust conditions, hence showing better DOC reactivity.



33x18mm (300 x 300 DPI)